J. Fluid Mech. (1987), *vol.* 176, *pp.* 357–378
Printed in Great Britain

The equilibrium shape and stability of menisci formed between two touching cylinders

By A. E. SÁEZ
Departamento de Termodinámica, Universidad Simón Bólivar,
P.O. Box 80659, Caracas 1080A, Venezuela

AND R. G. CARBONELL
Department of Chemical Engineering, North Carolina State University,
Raleigh, NC 27695-7905, USA

(Received 5 November 1985 and in revised form 30 July 1986)

The equilibrium shape and stability of menisci formed at the contact line between two vertically aligned cylinders were investigated by developing a general bifurcation analysis from the classic equation of Young–Laplace. It was found that the maximum amount of liquid that can be held at the contact line is determined by the existence of a bifurcation of the equilibrium solutions. The onset of instability is characterized by a translationally symmetric bifurcation that always precedes the instability to asymmetric perturbations. The maximum stable liquid retention is a strong function of the ratio of gravitational to surface-tension forces, indicating that gravity acts as a destabilizing force. The effect of contact angle on the maximum liquid retention is more complex: when the gravitational effects are small, an increase in contact angle results in a decrease in liquid retention; on the other hand, when the gravitational effects are appreciable, a maximum value of the liquid retention is obtained for intermediate values of the contact angle.

1. Introduction

There has recently been a renewed interest in the study of the shape and stability of fluid–fluid interfaces. The study of the mechanics of static menisci has applications in a wide variety of fields such as, for instance, oil recovery operations (Mohanty 1981), growth of crystals in zero-gravity liquid zones (Carruthers & Grasso 1972) and extrusion coating (Higgins & Brown 1984). An extensive review of the literature on the subject was recently presented by Michael (1981).

Much of the effort devoted to the study of solutions to the equation describing interface shapes (equations of Young–Laplace) has been concerned with the analysis of menisci related to microscopic phenomena, for which gravitational forces are negligible. For example, Erle, Dyson & Morrow (1971) studied the case of liquid bridges formed between separate cylinders and spheres, and Orr, Scriven & Rivas (1975) considered the case of the meniscus formed between a sphere and a flat plate. The inclusion of gravitational forces somewhat complicates the mathematical analysis.

A classical problem in which gravity is important is the determination of shapes and stability of pendent drops. This problem has been extensively studied mathematically by Pitts (1974, 1976), Michael & Williams (1976), Concus & Finn (1979) and Majumdar & Michael (1976, 1980). Majumdar & Michael (1980) showed that two-dimensional pendent drops become unstable to disturbances at a point of maximum volume with respect to changes in the internal pressure. These investigators also analysed the stability of the drop with respect to three-dimensional disturbances.

Boucher, Evans & McGarry (1982) recently studied the effects of gravity on the shape of menisci formed between flat plates for prescribed values of the contact angle.

The advances in the field of bifurcation theory (see, e.g. Thompson 1979) have been a source of mathematical tools for the description and analysis of meniscus stability, which has nowadays acquired a rigorous character. There are two different ways in which the stability analysis can be performed. First, the problem of finding the location and shape of the meniscus can be formulated as a minimum-energy problem, for which the equation of Young–Laplace is derived as the Euler–Lagrange condition of the variational formulation. In this case, the stability to small perturbations is studied following the classical approach of the calculus of variations, as described by Michael (1981). An alternative procedure is to introduce a perturbation to the equilibrium shape directly in the equation of Young–Laplace and then derive the criteria for the existence of a bifurcation; i.e. a second solution that is close to the equilibrium shape (see, e.g. Higgins & Brown 1984). These two approaches are based on the fact that the existence of bifurcating configurations implies that the meniscus is not physically feasible, since a small external perturbation would lead to the evolution of alternative shapes and, eventually, to the break-up of the interface. This idea has been experimentally supported by several investigations (e.g. Erle *et al.* 1971, and Kovitz 1975).

In this work we examine the equilibrium shape and stability of menisci formed at the contact line between two infinite, vertically aligned cylinders. We base the stability analysis on the introduction of a smooth, weak perturbation to the equilibrium shape in the two-dimensional equation of Young–Laplace. This leads to the governing equations for the perturbation function and then to the criteria that have to be satisfied for the existence of a bifurcating solution. The analysis is performed in a general way, in order to establish criteria for the stability of the equilibrium shape to perturbations that keep the volume of the liquid constant and perturbations that keep the internal pressure constant. An important result of the present study is the maximum amount of liquid that can be retained by a stable configuration. This parameter is related in this work to the contact angle and to the strength of the gravitational forces relative to surface-tension forces.

2. Problem formulation

Let us consider two touching cylinders of infinite length aligned vertically, as shown in figure 1. A certain amount of liquid (β-phase) is retained at the contact line between the cylinders, separated from the gas (γ-phase) by a phase interface whose spatial description is termed the 'meniscus'. The pressure distribution in the liquid phase under static conditions in dimensionless form is given by

$$P_\beta = P_{\beta 0} - y, \tag{1}$$

where P_β is the dimensionless pressure

$$P_\beta \equiv \frac{P'_\beta}{\rho_\beta g R}, \tag{2}$$

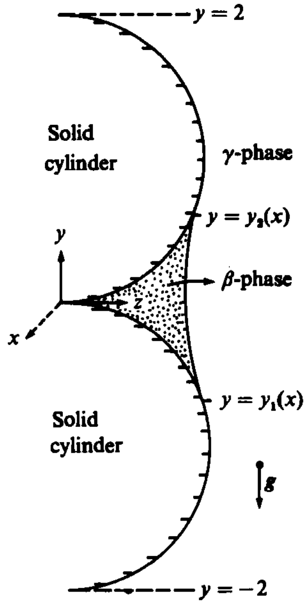

FIGURE 1. Liquid meniscus suspended between two parallel cylinders aligned vertically in the direction of gravity.

and y is the dimensionless y-coordinate

$$y = \frac{y'}{R}. \tag{3}$$

In these equations R is the radius of the cylinder. The parameter $P_{\beta 0}$ is the dimensionless pressure of the liquid at the level $y = 0$. The primes represent variables with dimensions.

Under the assumptions of negligible surface-tension gradients along the gas–liquid interface and low density of the gas with respect to the density of the liquid ($\rho_\gamma \ll \rho_\beta$), a force balance at the interface yields the well-known equation of Young–Laplace,

$$(E\ddot{o})\,P_\beta + 2H = 0, \tag{4}$$

where the pressure of the gas phase has been taken equal to zero as a datum level and the Eötvös number is defined by

$$E\ddot{o} = \frac{\rho_\beta g R^2}{\sigma}, \tag{5}$$

where σ is the surface tension of the β-phase. In (4), H is the dimensionless mean curvature which is related to the meniscus shape by (see Aris 1962)

$$2H = \frac{f_{xx}(1+f_y^2) - 2f_x f_y f_{xy} + f_{yy}(1+f_x^2)}{(1+f_x^2+f_y^2)^{\frac{3}{2}}}, \tag{6}$$

where $z = f(x, y)$ is the location of the gas–liquid interface and the subindices represent partial differentiation.

At the wetting lines ($y = y_1(x), y = y_2(x)$) the angle at which the meniscus intersects the solid surface, ϕ, is a property related to the interfacial tensions between the phases and it is geometrically determined by the shapes of the meniscus and the solid surface,

$$\cos\phi = \boldsymbol{n}_s \cdot \boldsymbol{n}_f \quad \text{at} \quad y = y_1(x), y_2(x), \tag{7}$$

where $\boldsymbol{n}_s$ and $\boldsymbol{n}_f$ are unit vectors normal to the solid surface and the meniscus respectively. If $z = S(x,y)$ represents the equation for the surface of the cylinders in dimensionless form, we have

$$S = \begin{cases} [1-(1+y)^2]^{\frac{1}{2}} & (-2 \leqslant y \leqslant 0), \\ [1-(1-y)^2]^{\frac{1}{2}} & (0 \leqslant y \leqslant 2). \end{cases} \tag{8}$$

Note that S is only a function of y owing to the translational symmetry of the cylinders.

The unit vectors $\boldsymbol{n}_s$ and $\boldsymbol{n}_f$ can be related to f and S by means of the following equations:

$$\boldsymbol{n}_s = \frac{1}{(1+S_y^2)^{\frac{1}{2}}}[-S_y \boldsymbol{e}_y + \boldsymbol{e}_z], \tag{9}$$

$$\boldsymbol{n}_f = \frac{1}{(1+f_x^2+f_y^2)^{\frac{1}{2}}}[-f_x \boldsymbol{e}_x - f_y \boldsymbol{e}_y + \boldsymbol{e}_z]. \tag{10}$$

The combination of (1), (4) and (6) leads to a partial differential equation for the meniscus shape f,

$$\frac{f_{xx}(1+f_y^2) - 2f_x f_y f_{xy} + f_{yy}(1+f_x^2)}{(1+f_x^2+f_y^2)^{\frac{3}{2}}} = (E\ddot{o})\, y - \lambda, \tag{11}$$

where

$$\lambda = P_{\beta 0}(E\ddot{o}) \tag{12}$$

can be considered as a dimensionless datum or reference pressure. On the other hand, the combination of (7), (9) and (10) leads to the boundary conditions that f has to satisfy at the wetting lines,

$$\cos\phi = \frac{(1+S_y f_y)}{(1+S_y^2)^{\frac{1}{2}}(1+f_x^2+f_y^2)^{\frac{1}{2}}} \quad \text{at} \quad y = y_1(x), y_x(x). \tag{13}$$

Furthermore, the meniscus and the solid surface intersect at the wetting lines, i.e.

$$f = S \quad \text{at} \quad y = y_1(x), y_2(x). \tag{14}$$

We shall restrict the present analysis to the family of shapes having reflective planes of symmetry along the x-axis, i.e. menisci whose shape is periodic in the x-direction with dimensionless wavelength equal to $2l$. This constraint imposes the following boundary conditions on f:

$$f_x = 0 \quad \text{at} \quad x = \pm l. \tag{15}$$

These conditions are physically equivalent to the case in which the meniscus intersects two surfaces parallel to the (z, y)-plane, located at $x = \pm l$, at right angles.

Equations (11), (13), (14) and (15) can be solved to find the meniscus shape f for given values of the Eötvös number, the dimensionless reference pressure λ and the contact angle. We will first focus our attention on the determination of translationally symmetric equilibrium shapes and afterwards we shall develop a general analysis based on perturbation methods to determine the stability of these configurations.

2.1. *Equilibrium shapes*

Let us consider that there exist equilibrium shapes that satisfy the set of equations presented above and that posess translational symmetry along the x-axis. In this case, the interface shape f will be a function of y only, described by the following equations:

$$\frac{f_{yy}}{[1+f_y^2]^{\frac{3}{2}}} = (E\ddot{o})\,y-\lambda, \tag{16}$$

$$\cos\phi = \frac{(1+f_y S_y)}{(1+S_y^2)^{\frac{1}{2}}(1+f_y^2)^{\frac{1}{2}}} \quad \text{at} \quad y = y_1, y_2 \tag{17}$$

and

$$f = S \quad \text{at} \quad y = y_1, y_2. \tag{18}$$

In this particular case the derivatives with respect to y are total derivatives and the y-coordinates of the wetting lines (y_1 and y_2) are independent of x.

Equation (17) can be expressed in a more manageable way by defining

$$\theta_f = \tan^{-1} f_y, \tag{19}$$

$$\theta_s = \tan^{-1} S_y, \tag{20}$$

where θ_f and θ_s are angles in the interval $(-\frac{1}{2}\pi, +\frac{1}{2}\pi)$. By using these definitions, (17) leads to

$$\phi = |\theta_f - \theta_s| \quad \text{at} \quad y = y_1, y_2, \tag{21}$$

in which we have taken into account the common convention that the contact angle ϕ is measured through the liquid phase, β.

In the absence of gravitational effects ($E\ddot{o} = 0$), the above equations can be solved analytically to obtain

$$f = S_1 + \frac{1}{\lambda}[(1-\lambda^2 y^2)^{\frac{1}{2}} - (1-\lambda^2 y_1^2)^{\frac{1}{2}}], \tag{22}$$

where S_1 is the value of S at $y = y_1$. Notice that if $\lambda = 0$ the above equation reduces to

$$f = S_1, \tag{23}$$

which corresponds to the simple case of a flat interface.

In any case where $E\ddot{o} = 0$ the shape of the meniscus is symmetric about $y = 0$, so that

$$y_2 = -y_1. \tag{24}$$

For given values of ϕ and λ, the wetting-line coordinates are not known *a priori* but they can be determined by introducing the derivative of the interface shape given by (22) into the equation

$$\tan\phi = \frac{f_{y1} - S_{y1}}{1 + S_{y1} f_{y1}} \tag{25}$$

obtained from (21) at $y = y_1$ and the definitions (19) and (20). Equation (25) is a nonlinear algebraic equation that in the present work is solved by Newton's method. In the particular case in which $\phi = 0$, this equation takes the simple form

$$y_1 = \frac{1}{\lambda - 1}. \tag{26}$$

When the Eötvös number is different from zero, (16), (18) and (21) do not have an analytical solution. In this case, the differential equation (16) was solved by a shooting method coupled with a Newton-type iterative procedure to locate the values of the boundary points y_1 and y_2. The equation was discretized by a fourth-order Runge–Kutta scheme.

2.2. *Stability*

2.2.1. *Fundamental analysis*

The translationally symmetric equilibrium shapes found by means of the procedure described above will not be stable if they can evolve to new equilibrium configurations when they are subjected to a smooth and weak perturbation. As we explained in §1, the existence of alternative shapes that are sufficiently close to the equilibrium menisci indicates that the calculated equilibrium shapes are not stable.

We start the stability analysis by proposing the existence of an alternative equilibrium configuration $f(x, y)$ that differs slightly from the translationally symmetric equilibrium shape $f^{(0)}(y)$,

$$f(x, y) = f^{(0)}(y) + \epsilon f^{(1)}(x, y) + O(\epsilon^2). \tag{27}$$

The parameter $\epsilon \ll 1$ restricts the new shape f to be the result of a weak perturbation to the basic shape $f^{(0)}$. In (27), $f^{(1)}$ is the perturbation to the equilibrium shape. In general, the perturbed solution may correspond to a perturbed value of the reference pressure,

$$\lambda = \lambda^{(0)} + \epsilon\lambda^{(1)} + O(\epsilon^2). \tag{28}$$

We now substitute (27) and (28) into (11) and then collect terms of $O(\epsilon^n)$ for $n = 0$ and 1. The terms of $O(\epsilon^0)$ lead to the equation

$$\frac{f_{yy}^{(0)}}{[1 + (f_y^{(0)})^2]^{\frac{3}{2}}} = (E\ddot{o})\, y - \lambda^{(0)}, \tag{29}$$

which is the governing equation for $f^{(0)}$, equivalent to (16).

The terms of $O(\epsilon)$ lead to

$$f_{xx}^{(1)}[1 + (f_y^{(0)})^2] + f_{yy}^{(1)} - 3[(E\ddot{o})\, y - \lambda^{(0)}] f_y^{(0)} [1 + (f_y^{(0)})^2]^{\frac{1}{2}} f_y^{(1)} = -\lambda^{(1)}[1 + (f_y^{(0)})^2]^{\frac{3}{2}}. \tag{30}$$

This is a linear, non-homogeneous partial differential equation for $f^{(1)}$, with variable coefficients.

At this point we need to find the boundary conditions that would allow the solutions of (29) and (30). In general, the equilibrium and perturbed shapes will not have the same wetting lines. Let us define Δy_i as the difference between the location of the wetting lines of each of the shapes,

$$\Delta y_i = y_i(x) - y_i^{(0)} \quad (i = 1, 2). \tag{31}$$

Notice that $y_i^{(0)}$ will not be a function of x owing to the translational symmetry of (29).

Since the perturbed shape differs at any point from the equilibrium shape by a term of order ϵ we assume that Δy_i must also be of order ϵ. In view of this, we can expand any function g about $y_i^{(0)}$ by means of the following Taylor series:

$$g(x, y_i) = g(x, y_i^{(0)}) + g_y(x, y_i^{(0)})\, \Delta y_i + O(\epsilon^2). \tag{32}$$

Let us also suppose that the perturbed shape $f(x, y)$ is defined in the region limited by the contact lines y_i and $y_i^{(0)}$. Notice that, if $|y_i| > |y_i^{(0)}|$, this will be the case, providing that the function f exists. On the other hand, if $|y_i| < |y_i^{(0)}|$, we are supposing that there exists a prolongation of f in the region $|y_i| < |y| < |y_i^{(0)}|$. With this in mind, the expansion (32) can be used to represent f in the region between the two wetting lines. Expanding f and S and substituting into the boundary condition (14) we get, neglecting terms of $O(\epsilon^2)$,

$$f(x, y_i^{(0)}) + f_y(x, y_i^{(0)})\,\Delta y_i = S(y_i^{(0)}) + S_y(y_i^{(0)})\,\Delta y_i. \tag{33}$$

Substituting (27) into (33) and collecting terms of the same order leads to

$$O(\epsilon^0):\quad f^{(0)}(y_i^{(0)}) = S(y_i^{(0)}), \tag{34}$$

$$O(\epsilon):\quad \Delta y_i = \frac{f^{(1)}(x, y_i^{(0)})\,\epsilon}{S_y(y_i^{(0)}) - f_y^{(0)}(y_i^{(0)})}. \tag{35}$$

Equation (34) is the same as boundary condition (18) for the symmetric shape and (35) allows one to express Δy_i in terms of ϵ.

In developing (34) and (35) we have considered the general case where $S_y(y_i^{(0)}) \neq f_y^{(0)}(y_i^{(0)})$. For the case of zero contact angle these two quantities are equal, according to (19), (20) and (21), and (33) leads to a simple boundary condition for $f^{(1)}$,

$$f^{(1)}(x, y_i^{(0)}) = 0 \quad (i = 1, 2); \quad \phi = 0, \tag{36}$$

which means that the perturbation leaves unchanged the location of the wetting lines.

For the case $\phi \neq 0$, (35) can be substituted into (32) to obtain a general expansion about $y_i^{(0)}$ of any function g,

$$g(x, y_i) = g(x, y_i^{(0)}) + \frac{\epsilon f^{(1)}(x, y_i^{(0)})\, g_y(x, y_i^{(0)})}{S_y(y_i^{(0)}) - f_y^{(0)}(y_i^{(0)})}. \tag{37}$$

The functions f and S can be expanded by means of this equation and the result can then be substituted into boundary condition (13). After some manipulations and collecting terms of the same order, the following results are obtained,

$$O(\epsilon^0):\quad \cos\phi = \frac{[1 + f_y^{(0)} S_y]}{(1 + S_y^2)^{\frac{1}{2}}\,[1 + (f_y^{(0)})^2]^{\frac{1}{2}}} \quad \text{at } y = y_1^{(0)}, y_2^{(0)}, \tag{38}$$

$$O(\epsilon):\quad \Omega_{1i} f_y^{(1)}(x, y_i^{(0)}) + \Omega_{2i} f^{(1)}(x, y_i^{(0)}) = 0 \quad (i = 1, 2), \tag{39}$$

where

$$\Omega_{11} = \frac{\tan\phi(1 + f_y^{(0)} S_y)}{1 + (f_y^{(0)})^2} \quad \text{at } y = y_1^{(0)}, \tag{40}$$

$$\Omega_{12} = -\frac{\tan\phi(1 + f_y^{(0)} S_y)}{1 + (f_y^{(0)})^2} \quad \text{at } y = y_2^{(0)}, \tag{41}$$

$$\Omega_{2i} = [1 + S_y(y_i^{(0)}) f_y^{(0)}(y_i^{(0)})]\left\{\frac{S_{yy}(y_i^{(0)})}{1 + S_y^2(y_i^{(0)})} - \frac{f_{yy}^{(0)}(y_i^{(0)})}{1 + [f_y^{(0)}(y_i^{(0)})]^2}\right\} \quad (i = 1, 2). \tag{42}$$

Equation (38) is equivalent to (17) and it represents the wetting-line boundary condition for the symmetric shape $f^{(0)}$. Equation (39) is a mixed-type boundary condition for $f^{(1)}$ and the parameters Ω_{ji} can be determined from a knowledge of $f^{(0)}$.

The boundary conditions at $x = \pm l$ (equation (15)), after substituting (27) lead to

$$f_x^{(1)}(x, y) = 0 \quad \text{at } x = \pm l, \tag{43}$$

since $f^{(0)}$ is translationally symmetric.

Summarizing, the perturbation to the equilibrium shape, $f^{(1)}(x, y)$, has to satisfy the differential equation, (30),

$$f_{xx}^{(1)}[1 + (f_y^{(0)})^2] + f_{yy}^{(1)} - 3[(E\ddot{o})\,y - \lambda^{(0)}] f_y^{(0)} [1 + (f_y^{(0)})^2]^{\frac{1}{2}} f_y^{(1)} = -\lambda^{(1)} [1 + (f_y^{(0)})^2]^{\frac{3}{2}}$$

and the following boundary conditions, (39), (43),

$$\Omega_{1i} f_y^{(1)}(x, y_i^{(0)}) + \Omega_{2i} f^{(1)}(x, y_i^{(0)}) = 0 \quad (i = 1, 2),$$

$$f_x^{(1)}(x, y) = 0 \quad \text{at} \quad x = \pm l.$$

Thus, the perturbation function has to satisfy a second-order, linear, non-homogeneous partial differential equation subject to homogeneous boundary conditions. The solution can be expressed as a sum of a particular solution to the non-homogeneous problem plus a homogeneous solution, as follows:

$$f^{(1)}(x, y) = P(y) + h(x, y). \tag{44}$$

The solution to the homogeneous part of the problem becomes simpler if the particular solution is forced to satisfy one of the conditions expressed by (39), say, the condition corresponding to $i = 2 (y = y_2^{(0)})$. Notice that P has been chosen to be a function of y only since the non-homogeneous term in (30) is only a function of y. According to this, we select a function P that satisfies the equations

$$P_{yy} - 3[(E\ddot{o})\, y - \lambda^{(0)}] f_y^{(0)} [1 + (f_y^{(0)})^2]^{\frac{1}{2}} P_y = -\lambda^{(1)} [1 + (f_y^{(0)})^2]^{\frac{3}{2}}, \tag{45}$$

$$\Omega_{12} P_y(y_2^{(0)}) + \Omega_{22} P(y_2^{(0)}) = 0. \tag{46}$$

Such a function is

$$P(y) = \lambda^{(1)} \left[\frac{\Omega_{11}}{\Omega_{22}} \gamma(y_2^{(0)}) + \Gamma(y_2^{(0)}) - \Gamma(y) \right], \tag{47}$$

where

$$\gamma(y) = y[1 + (f_y^{(0)})^2]^{\frac{3}{2}} \tag{48}$$

and

$$\Gamma(y) = \int_{y_1^{(0)}}^{y} \gamma(\xi)\, \mathrm{d}\xi. \tag{49}$$

In obtaining (47), use has been made of the differential equation for $f^{(0)}$, (29). According to (30), (39), (43) and (44) this choice of P results in the following set of equations for the homogeneous solution h:

$$h_{xx}[1 + (f_y^{(0)})^2] + h_{yy} - 3[(E\ddot{o})\, y - \lambda^{(0)}] f_y^{(0)} [1 + (f_y^{(0)})^2]^{\frac{1}{2}} h_y = 0, \tag{50}$$

with boundary conditions

$$\Omega_{11} h_y(y_1^{(0)}) + \Omega_{21} h(y_1^{(0)}) = \lambda^{(1)} [\Omega_{11} \gamma(y_1^{(0)}) - \frac{\Omega_{12}\Omega_{21}}{\Omega_{22}} \gamma(y_2^{(0)}) - \Omega_{21} \Gamma(y_2^{(0)})], \tag{51}$$

$$\Omega_{12} h_y(y_2^{(0)}) + \Omega_{22} h(y_2^{(0)}) = 0, \tag{52}$$

$$h_x(\pm l, y) = 0. \tag{53}$$

This set of equations can be solved by means of separation of variables, which yields a solution of the form

$$h(x, y) = \sum_{n=0}^{\infty} a_n u_n(x) v_n(y). \tag{54}$$

This technique leads to the following eigenvalue problem for $u_n(x)$:

$$(u_n)_{xx} + \xi_n^2 u_n = 0, \tag{55}$$

$$(u_n)_x(\pm l) = 0, \tag{56}$$

which yields

$$\xi_n = \frac{n\pi}{l} \quad (n = 0, 1, 2, 3, \ldots), \tag{57}$$

$$u_n(x) = \cos \frac{n\pi x}{l}. \tag{58}$$

The knowledge of the eigenvalues ξ_n leads to the following differential equation for $v_n(y)$:

$$(v_n)_{yy} - 3[(E\ddot{o})\,y - \lambda^{(0)}]f_y^{(0)}[1+(f_y^{(0)})^2]^{\frac{1}{2}}(v_n)_y - \frac{n^2\pi^2}{l^2}[1+(f_y^{(0)})^2]\,v_n = 0, \tag{59}$$

with boundary condition

$$\Omega_{12}(v_n)_y\,(y_2^{(0)}) + \Omega_{22}\,v_n(y_2^{(0)}) = 0. \tag{60}$$

The coefficients a_n in the series (54) are found by substituting (54) into boundary condition (51) and applying the orthogonality property of the family of functions $u_n(x)$. This leads to

$$a_0[\Omega_{11}(v_0)_y\,(y_1^{(0)}) + \Omega_{21}\,v_0(y_1^{(0)})] = \lambda^{(1)}[\Omega_{11}\,\gamma(y_1^{(0)}) - \frac{\Omega_{12}\,\Omega_{21}}{\Omega_{22}}\gamma(y_2^{(0)}) - \Omega_{21}\,\Gamma(y_2^{(0)})] \tag{61}$$

and

$$a_n[\Omega_{11}(v_n)_y\,(y_1^{(0)}) + \Omega_{21}\,v_n(y_1^{(0)})] = 0 \quad (n = 1, 2, \ldots). \tag{62}$$

The main objective of the present analysis is to find under which conditions the function $f^{(1)}$ is non-trivial. From a physical point of view, there are two different scenarios to consider. The first is the stability of the equilibrium shape to perturbations that keep the reference pressure constant. This would occur if, for example, there were a liquid-injection point at the contact line between the cylinders. The second corresponds to the stability of the equilibrium shape to perturbations that keep the volume of the meniscus constant, i.e. with no injection of liquid. From a mathematical point of view, constant-pressure perturbations mean $\lambda^{(1)} = 0$. The mathematical study of constant-volume perturbations requires further algebraic developments. First, let us define the dimensionless meniscus volume,

$$V_\beta = \frac{V'_\beta}{R^3} = \int_{-l}^{+l}\int_{y_1(x)}^{y_2(x)} (f-S)\,\mathrm{d}y\,\mathrm{d}x. \tag{63}$$

For the case of the translationally symmetric shape $f^{(0)}$, (63) reduces to

$$V_\beta^{(0)} = 2l\int_{y_1^{(0)}}^{y_2^{(0)}} [f^{(0)} - S]\,\mathrm{d}y. \tag{64}$$

The constant-volume constraint can be expressed as

$$V_\beta - V_\beta^{(0)} = 0. \tag{65}$$

We can subtract (64) from (63) and make use of (27). To evaluate the resulting expression, it is necessary to perform integrations in the interval $[y_i^{(0)}, y_i]$ with respect to y. Within this interval, the integrand can be approximated by means of the series expansion (37) which, for a general integrand $g(x,y)$, leads to

$$\int_{y_i^{(0)}}^{y_i} g(x,y)\,\mathrm{d}y = \frac{\epsilon f^{(1)}(y_i^{(0)})}{S_y(y_i^{(0)}) - f_y^{(0)}(y_i^{(0)})} \times\left\{g(x,y_i^{(0)}) + \tfrac{1}{2}g_y(x,y_i^{(0)})\left[2y_i^{(0)} + \frac{\epsilon f^{(1)}(y_i^{(0)})}{S_y(y_i^{(0)}) - f_y^{(0)}(y_i^{(0)})}\right]\right\}. \tag{66}$$

Using this equation and collecting terms of order-ϵ in (65) yields

$$\int_{-l}^{+l}\int_{y_1^{(0)}}^{y_2^{(0)}} f^{(1)}\,\mathrm{d}y\,\mathrm{d}x - y_2^{(0)}\int_{-l}^{+l} f^{(1)}(x,y_2^{(0)})\,\mathrm{d}x + y_1^{(0)}\int_{-l}^{+l} f^{(1)}(x,y_1^{(0)})\,\mathrm{d}x = 0. \tag{67}$$

This equation is the relation that $f^{(1)}$ has to satisfy in order to have a perturbed shape with the same volume as the equilibrium shape. This volume constraint can be further simplified by substituting (44), (47) and (54) into (67). After some manipulations this leads to

$$\int_{y_1^{(0)}}^{y_2^{(0)}} [a_0 v_0 - \lambda^{(1)}\Gamma]\,\mathrm{d}y - y_2^{(0)}[a_0 v_0(y_2^{(0)}) - \lambda^{(1)}\Gamma(y_2^{(0)})] = 0, \tag{68}$$

where $v_0(y)$ can be obtained by integrating (59),

$$v_0(y) = \int_{y_2^{(0)}}^{y} [1+(f_y^{(0)})^2]^{\frac{3}{2}}\,\mathrm{d}y - \frac{\Omega_{12}}{\Omega_{22}}[1+(f_y^{(0)}(y_2^{(0)}))^2]. \tag{69}$$

In the following subsections we will analyse each of the two stability scenarios separately.

2.2.2. *Stability to constant-pressure perturbations*

If the perturbations keep the reference pressure of the meniscus constant, then $\lambda^{(1)} = 0$ and the particular solution is, according to (47), $P(y) = 0$. Furthermore, the condition for a_0, (61), becomes homogeneous and we notice that a non-trivial solution for $f^{(1)}$ exists if, and only if, one of the factors multiplying a_n in (61) or (62) is identically equal to zero. This leads to the following condition for the instability of the basic shape $f^{(0)}$:

Condition I. An equilibrium shape, $f^{(0)}(y)$, is unstable to constant-pressure perturbations if there exists a number $\nu > 0$ such that there is a solution v to the problem

$$v_{yy} - 3[(E\ddot{o})\,y - \lambda^{(0)}]f_y^{(0)}[1+(f_y^{(0)})^2]^{\frac{1}{2}}v_y = \nu[1+(f_y^{(0)})^2]\,v, \tag{70}$$

$$\Omega_{12}\,v_y(y_2^{(0)}) + \Omega_{22}\,v(y_2^{(0)}) = 0, \tag{71}$$

that also satisfies

$$\Omega_{11}\,v_y(y_1^{(0)}) + \Omega_{21}\,v(y_1^{(0)}) = 0. \tag{72}$$

The basic shape will then be unstable to a perturbation of the form

$$f^{(1)}(x,y) = av(y)\cos(\nu^{\frac{1}{2}}x) \tag{73}$$

for any arbitrary value of a. Note that ν is related to the wavelength of the perturbation l by $\nu = n^2\pi^2/l^2$, according to (59) and (70).

Condition I leads to two physically different cases. First, if $\nu = 0$, the basic shape would be unstable to a translationally symmetric perturbation corresponding to the case $n = 0$, i.e.

$$f^{(1)} = a_0\left\{\int_{y_2^{(0)}}^{y} [1+(f_y^{(0)})^2]^{\frac{3}{2}}\,\mathrm{d}y - \frac{\Omega_{12}}{\Omega_{22}}[1+(f_y^{(0)}(y_2^{(0)}))^2]\right\}. \tag{74}$$

Since a_0 is arbitrary, the volume of the meniscus is not kept constant by this perturbation ((68) is not satisfied).

If $\nu > 0$, the non-symmetric part of the perturbation is characterized by wavelengths given by

$$l = \frac{n\pi}{\nu^{\frac{1}{2}}} \quad (n = 1, 2, \ldots). \tag{75}$$

Notice that $\nu > 0$ implies that, in general, $a_0 = 0$ (see (61) for $\lambda^{(1)} = 0$) and, therefore, this type of perturbation also keeps the volume of the meniscus constant since (68) is satisfied when $\lambda^{(1)}$ and a_0 are simultaneously equal to zero.

Condition I can be formulated as a Sturm–Liouiville eigenvalue problem. The differential operator in (70) can be transformed into its self-adjoint form by multiplying the equation by $q^{-\frac{3}{2}}$, where

$$q = 1+(f_y^{(0)})^2, \tag{76}$$

and making use of (29). The result is

$$[q^{-\frac{3}{2}}v]_y - \nu q^{-\frac{1}{2}}v = 0. \tag{77}$$

Thus, condition I can also be expressed as follows: the equilibrium shape $f^{(0)}(y)$ is unstable to constant-pressure perturbations if there exists a zero or negative eigenvalue ($\mu_m \leqslant 0$) for the following Sturm–Liouiville problem:

$$[q^{-\frac{3}{2}}v_m]_y + \mu_m q^{-\frac{1}{2}}v_m = 0, \tag{78}$$

$$\Omega_{12}(v_m)_y + \Omega_{22}v_m = 0 \quad \text{at } y = y_1^{(0)}, y_2^{(0)}. \tag{79}$$

This problem can be analysed by means of classical Sturm–Liouiville theory (see, e.g. Courant & Hilbert 1953). It can be shown that the eigenvalues can be expressed as

$$\mu_m = \frac{k_1 q(y_2^{(0)})^{-\frac{3}{2}}[v_m(y_2^{(0)})]^2 + k_0[q(y_1^{(0)})]^{-\frac{3}{2}}[v_m(y_1^{(0)})]^2 + \int_{y_1^{(0)}}^{y_2^{(0)}} q^{-\frac{3}{2}}(v_m)_y^2\,\mathrm{d}y}{\left[\int_{y_1^{(0)}}^{y_2^{(0)}} q^{-\frac{1}{2}}(v_m)^2\,\mathrm{d}y\right]}, \tag{80}$$

where

$$k_0 = -\Omega_{21}/\Omega_{11}, \tag{81}$$

$$k_1 = \Omega_{22}/\Omega_{12}. \tag{82}$$

The eigenvalues defined by (80) are the minimum of the expression on the right-hand side over the space of continuous and differentiable functions in the interval $[y_1^{(0)}, y_2^{(0)}]$, i.e.

$$\mu_m \leqslant \frac{k_1 q(y_2^{(0)})^{-\frac{3}{2}}[\Psi(y_2^{(0)})]^2 + k_0[q(y_1^{(0)})]^{-\frac{3}{2}}[\Psi(y_1^{(0)})]^2 + \int_{y_1^{(0)}}^{y_2^{(0)}} q^{-\frac{3}{2}}\Psi'^2\,\mathrm{d}y}{\int_{y_1^{(0)}}^{y_2^{(0)}} q^{-\frac{1}{2}}\Psi^2\,\mathrm{d}y}, \tag{83}$$

where Ψ is any continuous and differentiable function defined in $[y_1^{(0)}, y_2^{(0)}]$. According to this analysis, it is only necessary to find a function Ψ for which the expression on the right-hand side of (83) is negative to guarantee the existence of negative eigenvalues and, therefore, that the equilibrium shape is unstable. On the other hand, if k_0 and k_1 are greater than or equal to zero, it is obvious that there can be no negative eigenvalues and the basic shape is, therefore, stable. These two rules of simple inspection were enough to establish the stability of the shapes for some of the cases considered in this work. In order to obtain a more rigorous procedure applicable to all the possible cases, the calculations were performed by using the Rayleigh–Ritz technique in which the eigenvalues μ_m are found by expressing v_m in (80) in finite-difference form and using the power method to find the eigenvalues of the resulting algebraic system. The procedure is described in detail by Burden, Faires & Reynolds (1978).

2.2.3. *Stability to constant-volume perturbations with changes in the reference pressure*

Let us consider now the case in which $\lambda^{(1)} \neq 0$ and the perturbed shape satisfies the constant-volume constraint, (68). If we exclude from the analysis the solutions corresponding to constant-pressure perturbations, treated in the previous section, (61) and (62) lead to

$$a_0 = \lambda^{(1)}\frac{[\Omega_{11}\Omega_{22}\gamma(y_1^{(0)}) - \Omega_{12}\Omega_{21}\gamma(y_2^{(0)}) - \Omega_{21}\Omega_{22}\Gamma(y_2^{(0)})]}{\Omega_{22}[\Omega_{11}(v_0)_y(y_1^{(0)}) + \Omega_{21}v_0(y_1^{(0)})]}, \tag{84}$$

$$a_n = 0 \quad (n = 1, 2, \ldots). \tag{85}$$

Substituting (84) into (68), the volume constraint becomes

$$\int_{y_1^{(0)}}^{y_2^{(0)}} [\alpha_1 v_0 - \alpha_2 \Gamma]\,\mathrm{d}y - y_2^{(0)}[\alpha_1 v_0(y_2^{(0)}) - \alpha_2 \Gamma(y_2^{(0)})] = 0, \tag{86}$$

where

$$\alpha_1 = \Omega_{11}\Omega_{22}\gamma(y_1^{(0)}) - \Omega_{12}\Omega_{21}\gamma(y_2^{(0)}) - \Omega_{21}\Omega_{22}\Gamma(y_2^{(0)}), \tag{87}$$

$$\alpha_2 = \Omega_{22}[\Omega_{11}(v_0)_y(y_1^{(0)}) + \Omega_{21} v_0(y_1^{(0)})], \tag{88}$$

and $v_0(y)$ is given by (69).

It is interesting to point out that the new form of the volume constraint (86) is independent of the perturbation to the reference pressure $\lambda^{(1)}$. This analysis leads to a second condition for the instability of the equilibrium shape $f^{(0)}$.

Condition II. An equilibrium shape, $f^{(0)}(y)$, is unstable to constant-volume perturbations if it satisfies (86). The basic solution will be unstable to a perturbation of the form

$$f^{(1)}(y) = \lambda^{(1)}\left[\frac{\Omega_{11}}{\Omega_{22}}\gamma(y_2^{(0)}) + \Gamma(y_2^{(0)}) - \Gamma(y) + \frac{\alpha_1}{\alpha_2} v_0(y)\right]. \tag{89}$$

Equation (89) was obtained by combining (44), (47), (84) and (85). The resulting perturbation is translationally symmetric and directly proportional to the perturbation to the reference pressure.

Condition II can be evaluated once $f^{(0)}(y)$ has been determined by simply checking if it satisfies (86). This was done in the present work by evaluating the functions $v_0(y)$ and $\Gamma(y)$ numerically and then performing the numerical integration required in (86).

The procedures presented above were used to evaluate equilibrium shapes and their stability over a wide range of the independent parameters *Eö*, $\lambda^{(0)}$ and ϕ. The results are presented in the following section.

3. Results and discussion

According to the analysis presented in the previous section, there are three parameters that determine the shape of a meniscus formed at the contact line between two infinite cylinders: the Eötvös number *Eö*, the dimensionless reference pressure λ, and the contact angle ϕ. In this work we have calculated the equilibrium shapes corresponding to given sets of values of these parameters and then have checked the stability of those shapes by verifying whether they satisfied the conditions of instability. The results of these calculations are discussed below. First, we present the results corresponding to fixed values of the contact angle and then we perform a global comparison.

3.1. *The case of zero contact angle* ($\phi = 0$)

We have restricted the results to cases in which the meniscus touches the cylinders at two contact lines. This imposes a constraint on the maximum amount of liquid retained since it implies that the minimum value of y is -2 (see figure 1). In other words, we are not allowing for the presence of drops that hang from the cylinders. For $\phi = 0$ and in the absence of gravitational effects $E\ddot{o} = 0$, the meniscus of maximum volume intersects the cylinders at $y_1 = -2$ and it corresponds to a maximum value of the reference pressure of $\lambda = 0.5$, as shown in figure 2. As the reference pressure decreases, the volume of the liquid phase also decreases. The menisci shown in figure 2 are symmetric about $y = 0$ owing to the absence of gravitational effects. All the menisci corresponding to this case are stable since they do not satisfy the conditions of instability developed in the previous section.

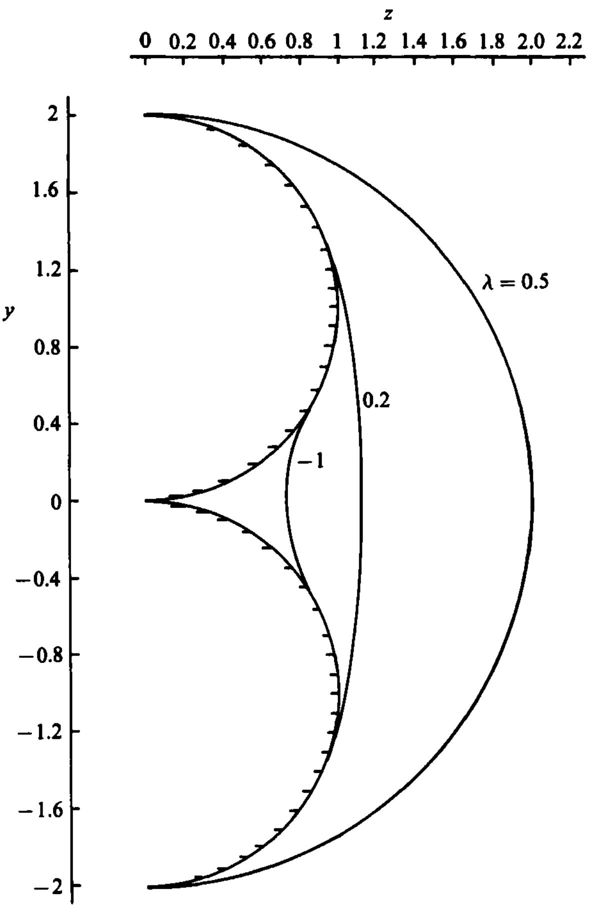

FIGURE 2. Shapes of the menisci for the case $E\ddot{o} = 0$ and $\phi = 0$.

As the Eötvös number is increased from zero, the meniscus of maximum volume intersects the lower cylinder at $y_1 = -2$ and the upper cylinder at a value $y_2 < 2$ that gradually decreases owing to the increases in the relative strength of the gravitational forces (the liquid tends to accumulate at the lower regions of the cylinder assembly). This behaviour is observed for values of $E\ddot{o}$ less than 0.5. When the Eötvös number reaches approximately 0.5, it is not possible to find a solution that intersects the lower cylinder at $y_1 = -2$. This is due to the geometrical impossibility of the solution to meet the lower cylinder at the location specified with a contact angle of zero. The value of y_1 corresponding to the meniscus of maximum volume is then limited by the Eötvös number and it becomes larger as $E\ddot{o}$ increases. The menisci of maximum volume as a function of the Eötvös number are shown in figure 3. The solutions of maximum volume with $y_1 > -2$ satisfy simultaneously the first condition of instability with $\nu = 0$ and the second condition. This means that the menisci shown in figure 3 with $E\ddot{o} > 0.5$ are unstable to translationally symmetric perturbations. However, a small decrease in the value of λ that generates those shapes leads to a very similar shape that is stable. This means that the maximum-volume shapes presented in figure 3 for $E\ddot{o} > 0.5$ are marginally unstable.

The shapes corresponding to $E\ddot{o} > 0$ (see figure 3) are not symmetric about $y = 0$.

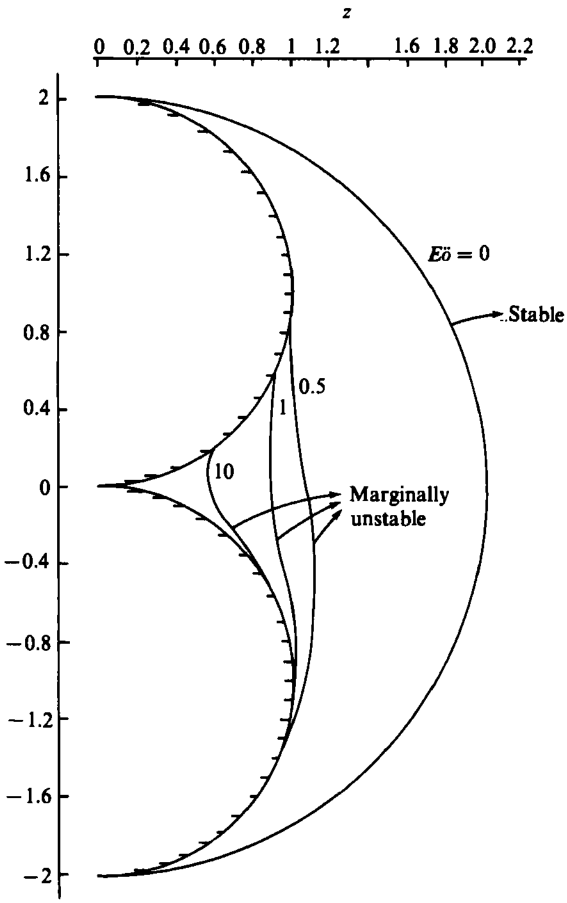

FIGURE 3. Menisci of maximum volume for the case $\phi = 0$ for various values of the Eötvös number.

As we mentioned before, the lower wetting line is displaced downwards owing to the effect of the gravitational pull.

The dimensionless volume of liquid per unit length is shown in figure 4 for $\phi = 0$ as a function of λ and the Eötvös number. For a given *Eö*, as the value of the reference pressure increases, the volume of the meniscus increases, reaching the limiting situation illustrated in figure 3 beyond which no solutions to the equilibrium equation can be obtained. It is interesting to point out that the dependence of $V_\beta/2l$ on λ is not affected by the Eötvös number, except in the range of λ close to the maximum volume limit.

3.2. *The case of contact angle* $\phi = \frac{1}{12}\pi$

A small increase in the contact angle to a value of $\frac{1}{12}\pi$ (15°) leads to appreciable changes in the behaviour of the liquid retention. It was found that, for a given value of the Eötvös number, there was a marginally stable shape corresponding to the meniscus of maximum volume that can exist physically. The shapes of these maximum-volume menisci are shown in figure 5 for various values of *Eö*. But, in contrast with the case of zero contact angle, there exist equilibrium shapes with larger volumes that satisfy the instability conditions. Figure 6 shows the reference pressure

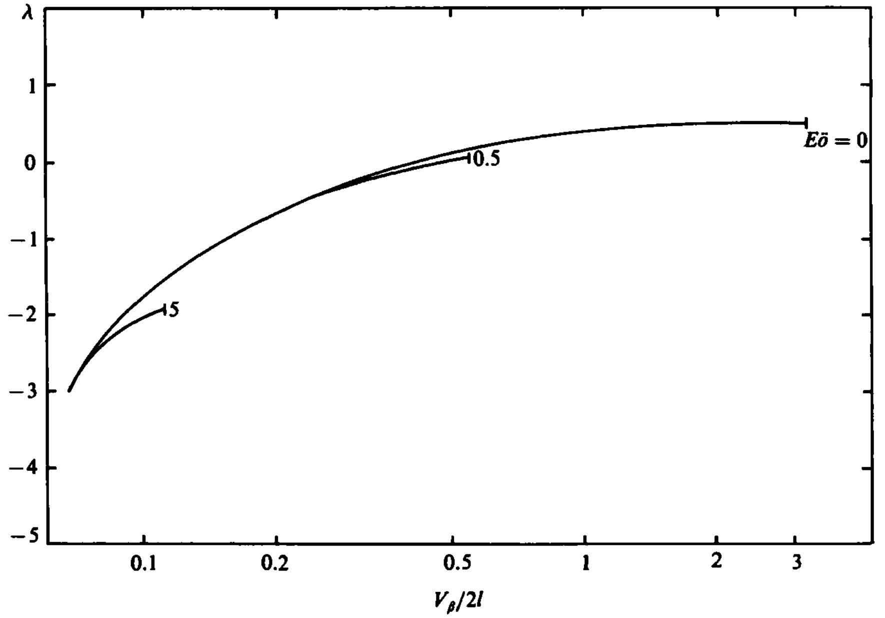

FIGURE 4. Volume of suspended menisci for the case $\phi = 0$ as a function of λ for various values of Eötvös number.

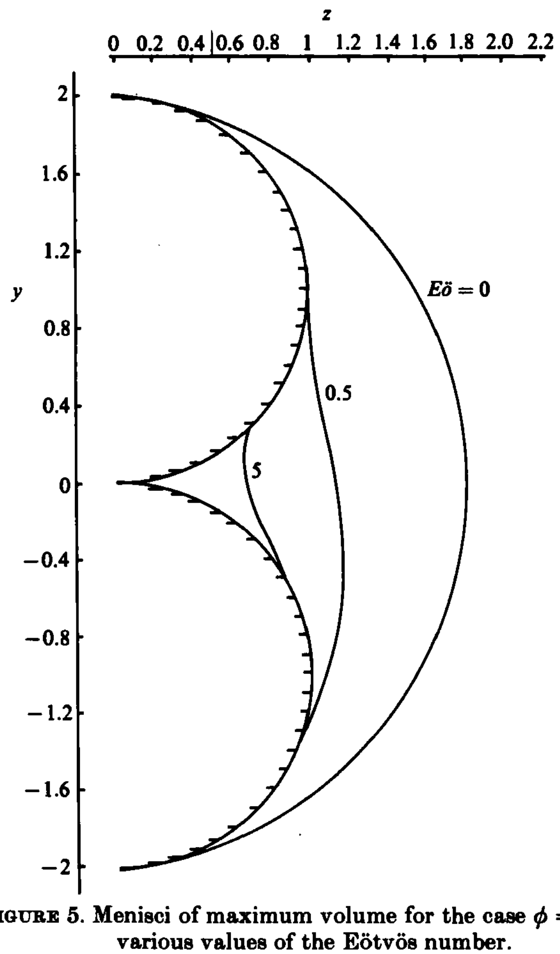

FIGURE 5. Menisci of maximum volume for the case $\phi = \frac{1}{12}\pi$ for various values of the Eötvös number.

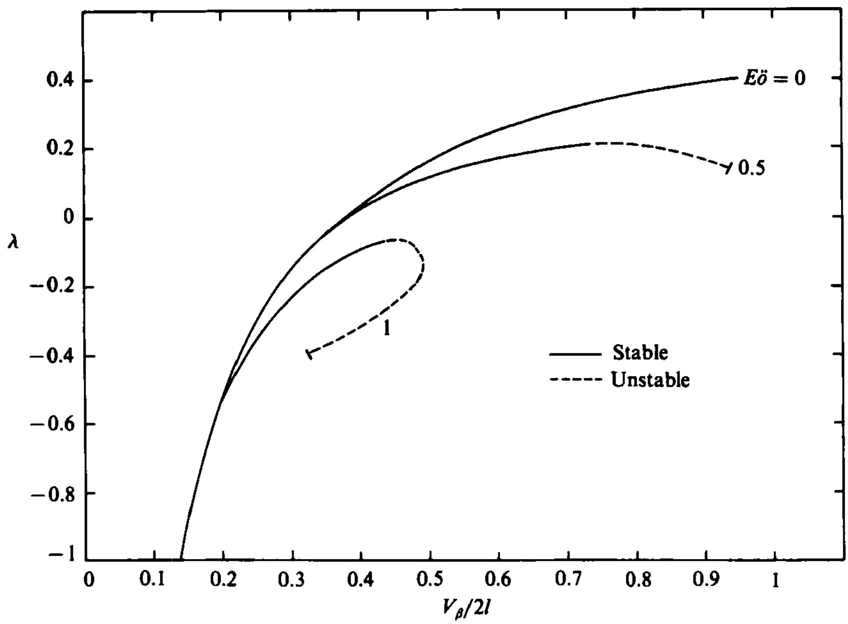

FIGURE 6. Volume of suspended menisci for the case $\phi = \frac{1}{12}\pi$ as a function of λ for various values of the Eötvös number.

as a function of the parameters $V_\beta/2l$ and $E\ddot{o}$, illustrating the existence of unstable shapes. At approximately the maximum value of λ (see figure 6), the meniscus satisfies simultaneously condition II and condition I with $\nu = 0$, indicating that it is unstable to translationally symmetric perturbations. Solutions of larger volumes than that corresponding to the onset of unstable behaviour are obtained, and they satisfy condition I with $\nu < 0$, indicating that these solutions are unstable to asymmetric perturbations. For large Eötvös number (for instance, $E\ddot{o} = 1$ in figure 6) there are unstable solutions with the same volume as stable ones but with different values of the reference pressure.

An example of the bifurcation of solutions for a given value of λ is presented in figure 7. The case considered ($\lambda = 0.13, E\ddot{o} = 0.5$) yields two different solutions to the equilibrium equation of which the shape with the largest volume is unstable to asymmetric perturbations.

3.3. *The case of contact angle* $\phi = \frac{1}{6}\pi$

The existence of a marginally stable shape corresponding to the maximum liquid retention is still observed as the contact angle is further increased. For $\phi = \frac{1}{6}\pi$ (30°) the maximum-volume shapes are presented in figure 8 as a function of the Eötvös number. Figure 9 shows the relation between the reference pressure and the liquid retention, showing a similar qualitative behaviour as the case $\phi = \frac{1}{12}\pi$.

The results obtained in this investigation show that there are two factors that limit the amount of liquid that can be retained at the contact point between two infinite and vertically aligned cylinders. First, there is a geometrical limitation imposed by the shape of the solid surface and the constraint $y_1 > -2$. This limits the solutions of the equilibrium equations (represented by bars in figures 4, 6 and 9) and it represents the maximum-volume meniscus attainable for the case with $\phi = 0$. For contact angles greater than zero, the maximum amount of liquid is determined by

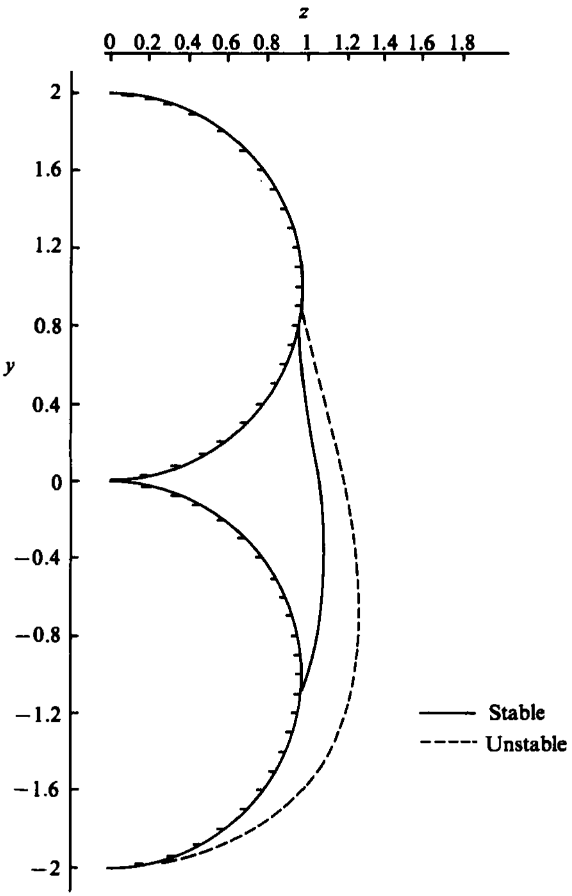

FIGURE 7. Two different bifuration solutions for the case $\lambda = 0.13, E\ddot{o} = 0.5$.

the onset of shape instability, according to the theoretical criteria developed in the present work. The stable menisci of maximum volume approximately correspond to a maximum in the value of the reference pressure, as observed in figures 4, 6 and 9. This result is consistent with the analysis presented by Pitts (1976), for the pendant drop geometry. The maximum reference pressure is presented in figure 10 as a function of the Eötvös number for various values of the contact angle.

The maximum volume that can exist physically is presented in figure 11 as a function of the contact angle for fixed values of the Eötvös number. When the surface-tension forces are much larger than the gravitational forces ($E\ddot{o} \rightarrow 0$), the maximum volume decreases as the contact angle increases. For appreciable gravitational effects (for instance, $E\ddot{o} = 1.5$, see figure 11), the volume exhibits a maximum with respect to the contact angle and it shows a decreasing trend for relatively large values of this parameter. This behaviour is caused by two opposite effects. First, low contact angles mean, in general, stable shapes extended over large areas of the solid surface (better wetting characteristics), this can be seen by comparing figures 3, 5 and 8. Secondly, low contact angles also imply that the meniscus has a shape that is closer point by point to the surface of the cylinders, compared to that obtained for large contact angles. The relative importance of these effects can be clearly appreciated in figure 12, where the interface shapes corresponding to the menisci of

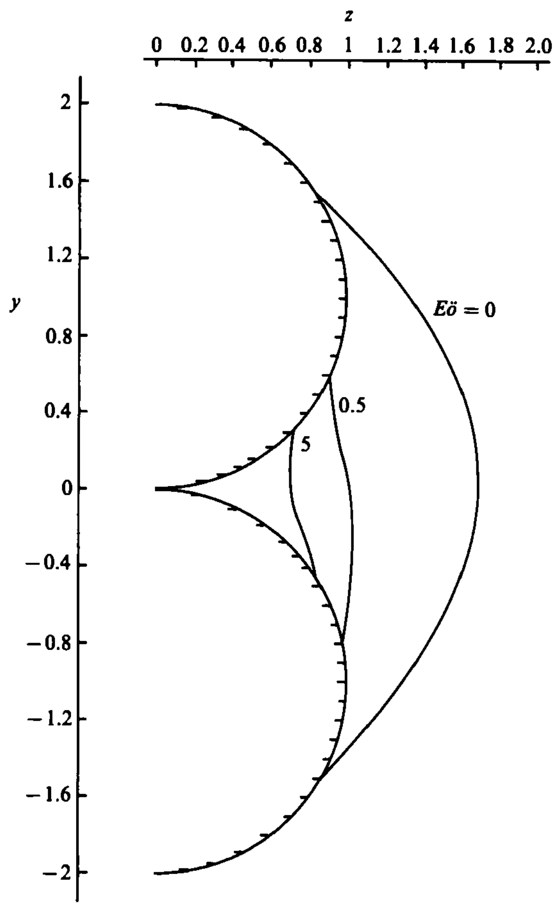

FIGURE 8. Menisci of maximum volume for the case $\phi = \frac{1}{6}\pi$ for various values of the Eötvös number.

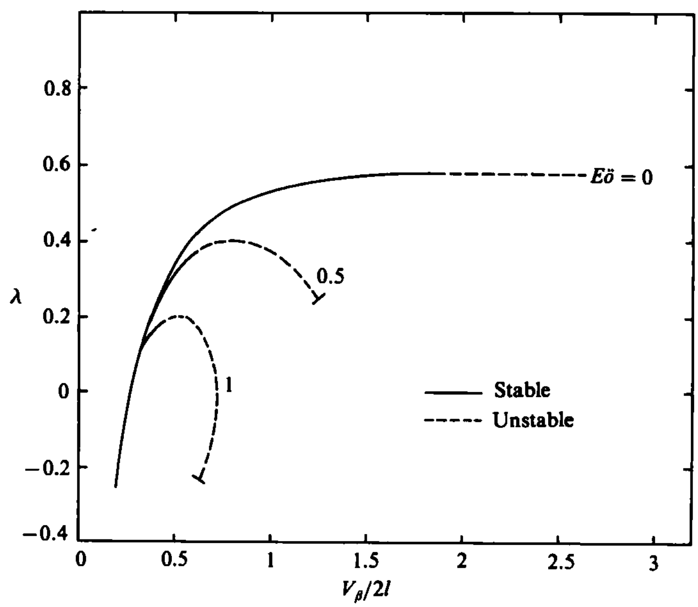

FIGURE 9. Volume of suspended menisci for the case $\phi = \frac{1}{6}\pi$ as a function of λ for various values of the Eötvös number.

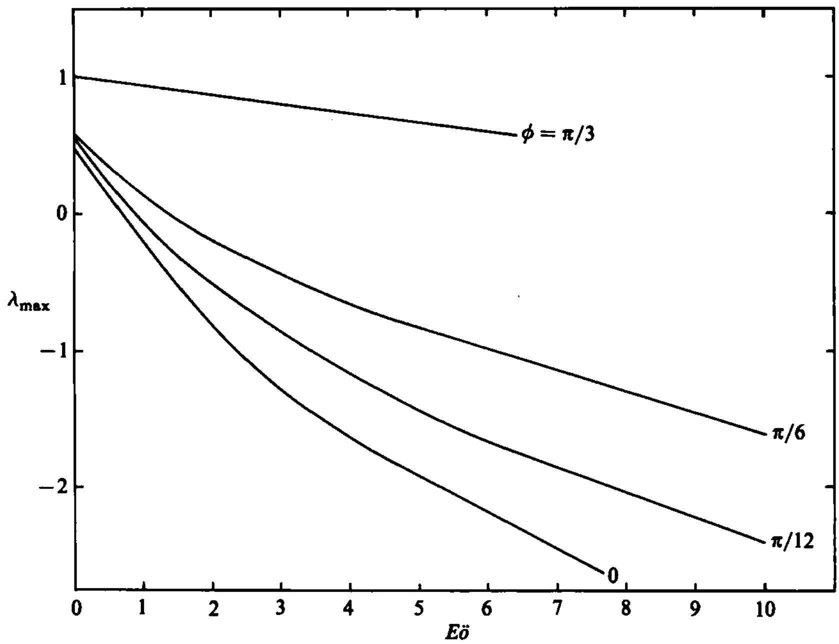

FIGURE 10. Maximum value of the reference pressure as a function of the Eötvös number for different contact angles.

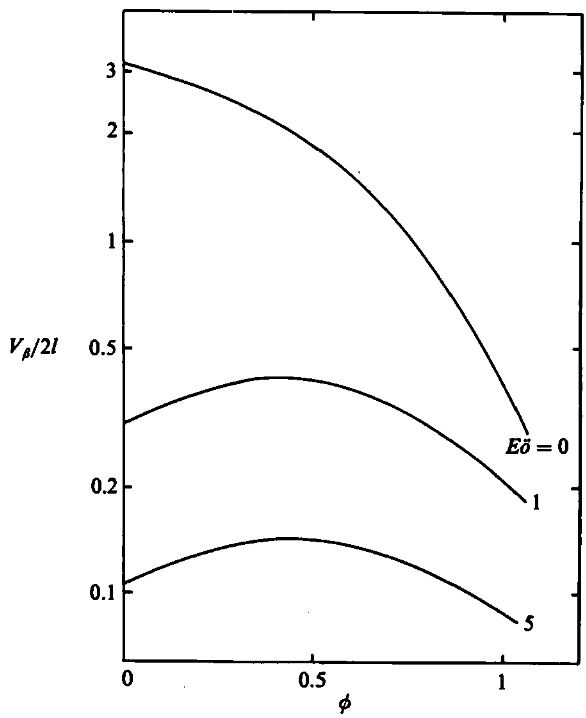

FIGURE 11. Maximum volume of liquid suspended as a function of the contact angle for various Eötvös numbers.

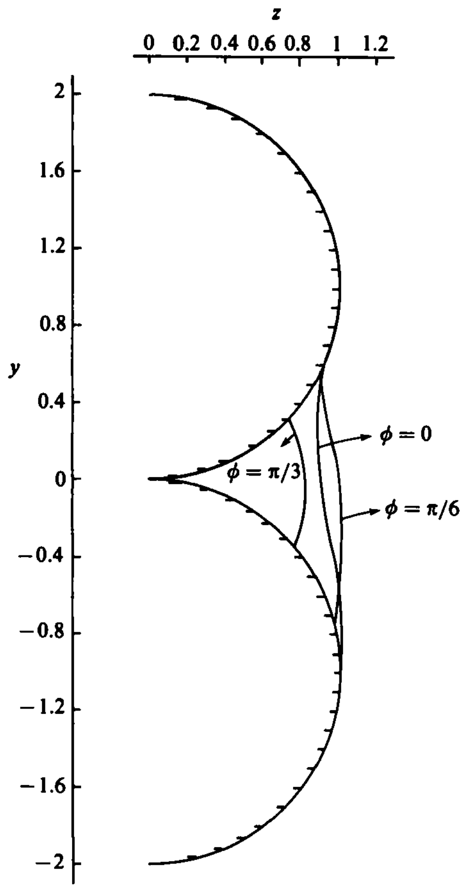

FIGURE 12. Menisci of maximum volume for the case $E\ddot{o} = 1$ for various contact angles.

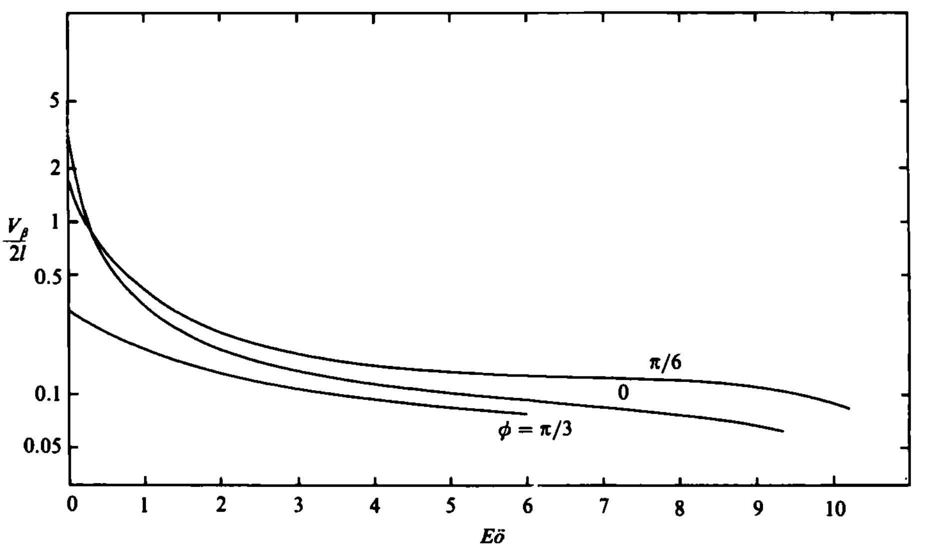

FIGURE 13. Maximum volume of liquid suspended as a function of the Eötvös number for different contact angles.

maximum volume are presented for $Eö = 1$ as a function of the contact angle. As the contact angle is increased from 0 to $\frac{1}{6}\pi$, there is a slight decrease in the wetted area but an increase in the volume owing to the greater separation of the interface from the solid induced by the larger contact angle. Further increases in the contact angle lead to lower wetted areas until the effect of this trend on the volume overwhelms that caused by the separation of the interface.

The maximum volumes of stable menisci are presented in figure 13 as a function of the Eötvös number for several values of the contact angle. This figure shows that an increase in the relative strength of the gravitational forces with respect to surface-tension forces (larger $Eö$) produces a destabilizing effect on the liquid phase that results in a decrease in the maximum liquid retention.

The analysis developed in the present investigation gives an idea of the trends followed by the liquid retention as a function of Eötvös number in complex structures made up of cylinders or particles in which all the retention occurs at the contact points. The trend observed in figure 13 is consistent with experimental observations of liquid retention in porous media (see Sáez 1984).

4. Conclusions

The amount of liquid retained at the contact line between two infinite and vertically aligned cylinders is appreciably affected by three independent parameters: a datum (reference) level of the pressure in the liquid phase, the contact angle and the relative strength of gravitational and surface-tension forces. The analysis developed in this work has shown that, for specified values of the Eötvös number and the contact angle, there is a unique configuration that determines the maximum amount of liquid that can be held at the contact line between the cylinders. This maximum liquid retention is determined by stability considerations, except for low values of the Eötvös number ($Eö < 0.5$) and zero contact angle where geometrical effects are dominant.

The gravitational force has a destabilizing effect on the menisci which produces a lower maximum volume of liquid as the Eötvös number increases. On the other hand, the effect of the contact angle is two-fold: an increase in this parameter leads to lower values of the wetted areas but larger separation between the menisci and the solid surface. These two effects result in the existence of increasing and decreasing trends of the maximum retention as the contact angle increases.

The onset of unstable behaviour is controlled by the bifurcation of the equilibrium shapes to translationally symmetric shapes, a product of symmetric perturbations. In all the results obtained in this work, symmetric instabilities are always preceded by asymmetric bifurcations.

This work was supported in part by a grant from Chevron Research Co. One of the authors (A. E. Sáez) was supported by a fellowship from FONINVES of Venezuela.

REFERENCES

ARIS, R. 1962 Vectors, tensors, and the basic equations of fluid mechanics. Prentice Hall.

BOUCHER, E. A., EVANS, M. J. B. & McGARRY, S. 1982 Capillary phenomena. XX. Fluid bridges between horizontal solid plates in a gravitational field. *J. Colloid Interface Sci.* **89**, 154.

BURDEN, R. L., FAIRES, J. D. & REYNOLDS, A. C. 1978 *Numerical Analysis*, 2nd edn. Prindle, Webber & Schmidt.

CARRUTHERS, J. R. & GRASSO, M. 1972 Studies of floating liquid zones in simulated zero gravity. *J. Appl. Phys.* **43**, 436.

CONCUS, P. & FINN, R. 1979 The shape of a pendent liquid drop. *Phil. Trans. R. Soc. Lond.* A **292**, 307.

COURANT, R. & HILBERT, D. 1953 *Methods of Mathematical Physics*, vol. 1. Wiley.

ERLE, M. A., DYSON, D. C. & MORROW, W. R. 1971 Liquid bridges between cylinders, in a torus, and between spheres. *AIChE J.* **17**, 115.

HIGGINS, B. G. & BROWN, R. A. 1984 Multiple equilibrium shapes of partially constrained menisci: a quasi-static mechanism for instability of a coating bead. *Chem. Engng Sci.* **39**, 1339.

KOVITZ, A. A. 1975 Static fluid interfaces external to a right circular cylinder – experiment and theory. *J. Colloid Interface Sci.* **50**, 125.

MAJUMDAR, S. R. & MICHAEL, D. H. 1976 The equilibrium and stability of two dimensional pendent drops. *Proc. R. Soc. Lond.* A **351**, 89.

MAJUMDAR, S. R. & MICHAEL, D. H. 1980 The instability of plane pendent drops. *J. Colloid Interface Sci.* **73**, 186.

MICHAEL, D. H. 1981 Meniscus stability. *Ann. Rev. Fluid Mech.* **13**, 189.

MICHAEL, D. H. & WILLIAMS, P. G. 1976 The equilibrium and stability of axisymmetric pendent drops. *Proc. R. Soc. Lond.* A **351**, 117.

MOHANTY, K. K. 1981 Fluids in porous media: two-phase distribution and flow. Ph.D. dissertation, University of Minnesota.

ORR, F. M., SCRIVEN, L. E. & RIVAS, A. P. 1975 Pendular rings between solids: meniscus properties and capillary force. *J. Fluid Mech.* **67**, 723.

PITTS, E. 1974 The stability of pendent liquid drops. Part 2. Axial symmetry. *J. Fluid Mech.* **63**, 487.

PITTS, E. 1976 The stability of a drop hanging from a tube. *J. Inst. Maths Applics* **17**, 387.

SÁEZ, A. E. 1984 Hydrodynamics and lateral thermal dispersion for gas–liquid cocurrent flow in packed beds. Ph.D. dissertation, University of California, Davis.

THOMPSON, J. M. T. 1979 Stability predictions through a succession of folds. *Phil. Trans. R. Soc. Lond.* A **292**, 1.